Direct observation of capsaicin-induced intramolecular dynamics of TRPV1 channel

The transient receptor potential vanilloid type 1 (TRPV1) is a multimodal receptor that responds to various stimuli such as the chemical ligand capsaicin (a component of chili peppers), protons (H^+), and a physical stimulus of heat (high temperature). Professor David Julius was awarded the 2021 Nobel Prize in Physiology or Medicine for his discovery of the TRPV1 channel. Recent advances in cryoelectron microscopy (cryo-EM) have revealed the detailed structures of TRPV1. In addition to its apo structure (ligand-unbound), capsaicin-bound structures and a complex with a spider toxin DkTx and with a highly potent capsaicin analogue RTX have been reported. However, because of the large size of TRPV1 (400 kDa) and the complexity of its structure, the real-time motion of channel gating has not been well documented. Information about the intramolecular dynamics, as well as structural information, is necessary to understand the molecular mechanisms of protein functions. In this study, we applied diffracted X-ray tracking (DXT) to purified TRPV1 protein and successfully visualized its capsaicin-induced intramolecular torsional motion [1].

DXT uses fine gold nanocrystals with a diameter of 20–60 nm as quantum probes. Domains of the target proteins were chemically labeled by the gold nanocrystals, and their motion (orientation) was tracked as X-ray Laue spots with microsecond time resolution (Fig. 1(a)). Professor Yuji C. Sasaki designed this technique in 1997 and demonstrated it in 2000 at SPring-8 [2]. DXT can be measured under various solution conditions of pH and temperature, and this is one of the single-molecule motion measurement techniques with ultrahigh spatiotemporal resolution [3,4]. DXT can be used with various X-ray sources from large synchrotron radiation facilities to ordinary laboratory X-ray generators [5]. To measure the movement of diffracted spots from nanocrystals, we used the high-flux beamline SPring-8 **BL40XU** with a wide energy bandwidth ($\Delta E/E = 0.08$) for DXT. To prevent damage to the sample, the exposure time was strictly controlled by synchronizing a galvanometer-type X-ray high-speed shutter and a low-noise X-ray image intensifier (Hamamatsu Photonics V5445P). A high-speed CMOS camera (Photron FASTCAM SA1.1) was used at a frame rate of 100 μs. One hundred frames were captured for each spot (Fig. 1(b)).

For the specific binding of gold nanocrystals, a Met-tag sequence (MGGMGGM) was introduced to a S1-S2 loop (for the "voltage-sensor-like-domain" label) or a S5-Pore loop (for the "pore-domain" label) of the TRPV1 proteins. The rotation angles of all the bright spots were analyzed separately at positive angles (counterclockwise axis direction; CCW) and negative angles (clockwise direction; CW) viewed from the top (extracellular) side. First, we observed the ligand effect on rotation bias. It was found that the rotation signals were evenly distributed on both sides, and no information about rotation bias was obtained. After some consideration about it, we concluded that rotational biases must be canceling out owing to the repetitive "twisting" and "untwisting" motion of each channel protein.

To segregate the opening and closing movement of TRPV1, a lifetime filtering technique was applied. Diffraction spots from gold nanocrystals can be recorded within the energy range of synchrotron radiation. The spots of fast-moving proteins have a short duration between appearance and disappearance, while those of slow-moving proteins exist for a long time. Hence, the duration of the bright spots represents the overall movement of the target protein (lifetime). Therefore, the data were divided into a short-lifetime group [lifetime (LT) < 2.5 ms], a medium-LT group [2.5 ≤ LT < 4 ms], and a long-LT group [8 ≤ LT < 10 ms], and statistical analysis was applied to each group independently (Fig. 2). This allowed us to detect the ligand-induced internal motions of TRPV1. The short-LT data were mostly nondirectional or slightly CW biased for both S5-P and S1-S2 loops. In the medium-LT group, both apo and capsaicin-bound TRPV1 showed CW bias, while AMG9810 was nondirectional (S5-P loop)

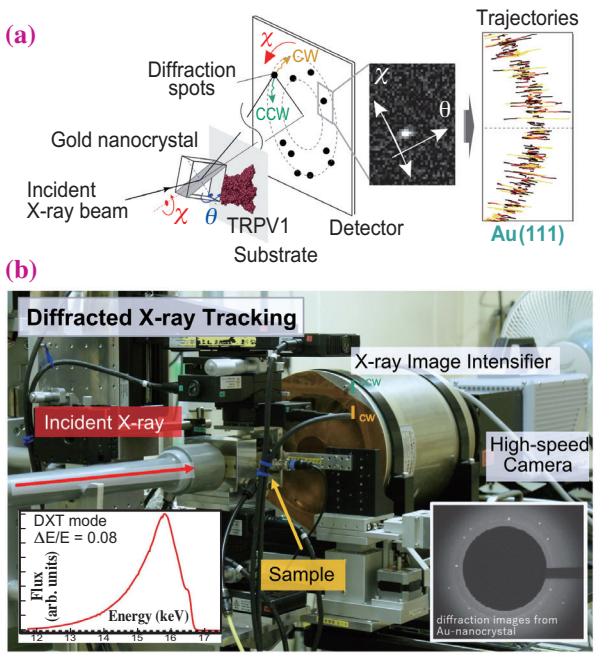

Fig. 1. DXT measurement system. **(a)** Schematic of the DXT data collection. Pink-beam X-rays from SPring-8 yielded trackable diffraction spots from the gold nanocrystals. The trajectories were separately projected and analyzed on $\chi-\theta$ coordinates. **(b)** DXT measurement system at BL40XU, and the X-ray spectrum of the incident beam measured by a PIN diode detector.

or CCW-biased (S1-S2 loop). The long-LT group exhibited CW bias for capsaicin, but CCW bias for apo-TRPV1. The CW torsional motion (observed for both apo and capsaicin-bound TRPV1) was considered to be channel opening motion from the cryo-EM observations. Although the obtained motions were extremely small, detailed information on the motions was obtained by the lifetime filtering method and theoretical calculations using the cryo-EM structure (Fig. 3). The diffusion constant of glycine 602 at the OP-labeled position was calculated to be 12.8 pm^2/ms. Interestingly, the channel antagonist AMG9810 generated the opposite torsional bias to that of capsaicin.

We also examined the motion of the capsaicin-insensitive Y511A mutant to confirm whether the CW bias is indeed related to gating. It is noteworthy that the torsional motion of the Y511A mutant was strongly biased in the CCW direction, which resembles well the AMG9810-induced CCW bias observed for the wild type. The TRPV1 channel has two gates in the ion pass; the upper gate is located on the extracellular side of the membrane and the lower gate on the cytoplasmic side. The capsaicin-bound structure presented by cryo-EM was a closed form, because the lower gate was opened and the upper gate was closed. Our DXT results showed that both apo and capsaicin-bound TRPV1 had a CW rotational bias, and this bias was observed even in the long-LT group bound by capsaicin. These results suggest that the main action of capsaicin is not only to open the lower gate, but also to increase the oscillation frequency at the upper gate by pulling a small trigger, thereby promoting calcium influx.

TRPV1 channels are abundantly expressed in primary sensory nerves such as unmyelinated C-fibers and myelinated small Aδ fibers, which act as nociceptors to induce pain and burning sensations. Therefore, search for new inhibitors from the viewpoint of analgesic drug development is anticipated. New insights gained from structural dynamism must be useful for understanding pain recognition mechanisms and developing new analgesics. Several TRP species have been reported to be closely related to the pathogenesis of diseases, and the DXT measurement technique can contribute widely to the discovery and understanding of therapeutic agents for these diseases.

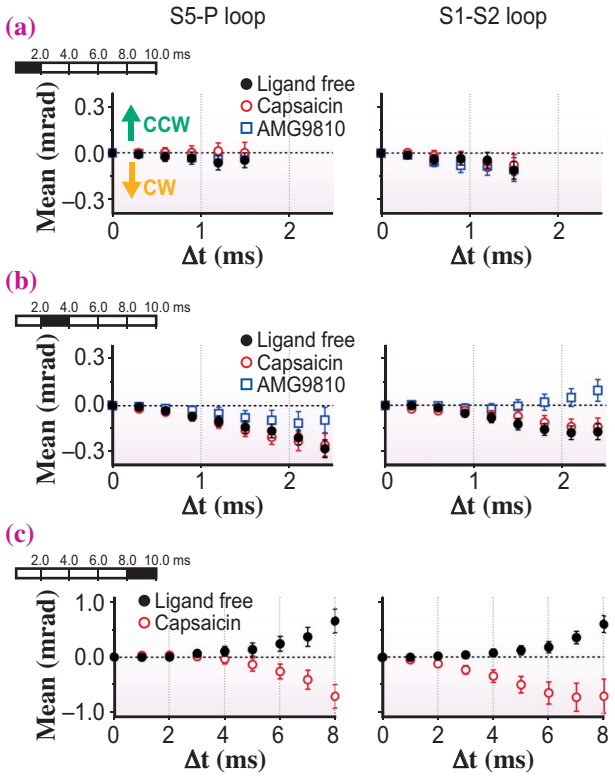

Fig. 2. Lifetime filtering analysis. Mean plot for angle χ for **(a)** data for short-LT group (< 2.0 ms), **(b)** medium-LT group (2.0 ≤ LT < 4.0 ms), and **(c)** long-LT group (8.0 ≤ LT < 10.0 ms). In the long-LT group, capsaicin-bound TRPV1 sustained CW bias, while apo-TRPV1 showed CCW bias.

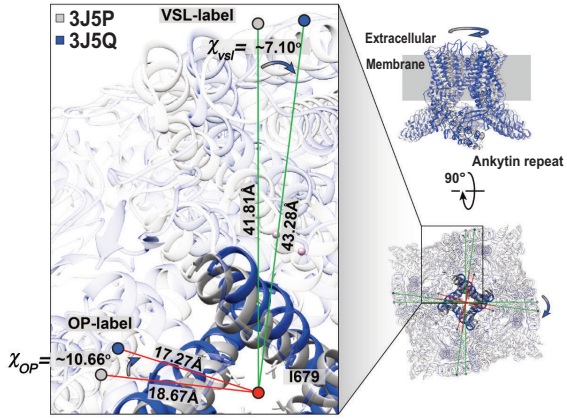

Fig. 3. Superimposed views of closed and open forms of TRPV1. Superimposition of apo-TRPV1 (PDB: 3J5P, gray) and DkTx/RTX-TRPV1 (3J5Q, blue). Rotational angles after DkTx/RTX binding were calculated at glycine 602 (OP-label) and tyrosine 463 (VSL-label). Both the OP and VSL positions rotated in the clockwise direction, resulting in 10.6 and 7.1 degrees, respectively.

Kazuhiro Mio[a,*], Shoko Fujimura[a] and Yuji C. Sasaki[a,b]

[a] OPERANDO-OIL, National Institute of Advanced Industrial Science and Technology (AIST)
[b] Graduate School of Frontier Sciences, The University of Tokyo

*Email: kazu.mio@aist.go.jp

References

[1] *S. Fujimura, K. Mio, M. Kuramochi, H. Sekiguchi, K. Ikezaki, M. Mio, K. Hengphasatporn, Y. Shigeta, T. Kubo, Y. C. Sasaki: J. Phys. Chem. B.* ***124*** *(2020) 11617.*
[2] Y.C. Sasaki *et al.*: Phys. Rev. E **62** (2000) 3843.
[3] H. Sekiguchi *et al.*: Sci. Rep. **4** (2014) 6384.
[4] K. Mio *et al.*: Biochem. Biophys. Res. Commun. **529** (2020) 306.
[5] H. Sekiguchi *et al.*: Sci. Rep. **8** (2018) 17090.